Radiative transfer modeling of a large pool fire by discrete ordinates, discrete transfer, ray tracing, Monte Carlo, and moment methods

By K. A. Jensen†, J.-F. Ripoll, A. A. Wray‡, D. Joseph¶ AND M. El Hafi¶

Five computational methods for solution of the radiative transfer equation in an absorbing-emitting and non-scattering gray medium were compared on a 2 m JP-8 pool fire. The temperature and absorption coefficient fields were taken from a synthetic fire due to the lack of a complete set of experimental data for fires of this size. These quantities were generated by a code that has been shown to agree well with the limited quantity of relevant data in the literature. Reference solutions to the governing equation were determined using the Monte Carlo method and a ray tracing scheme with high angular resolution. Solutions using the discrete transfer method, the discrete ordinate method (DOM) with both S_4 and LC_{11} quadratures, and moment model using the M_1 closure were compared to the reference solutions in both isotropic and anisotropic regions of the computational domain. DOM LC_{11} is shown to be the more accurate than the commonly used S_4 quadrature technique, especially in anisotropic regions of the fire domain. This represents the first study where the M_1 method was applied to a combustion problem occurring in a complex three-dimensional geometry. The M_1 results agree well with other solution techniques, which is encouraging for future applications to similar problems since it is computationally the least expensive solution technique. Moreover, M_1 results are comparable to DOM S_4.

1. Motivation and objectives

Accurate prediction of the heat flux to an object exposed in a large fire is important for consideration of the thermal hazard to engineered systems, personnel, and facilities. Such fires could potentially occur from a transportation accident. Fires of this scale have relatively low velocities and high temperatures, and therefore the majority of heat transfer to an object is dominated by the radiative emission from high-temperature soot (Gritzo *et al.* 1998). The computational cost for solution of the radiative transfer equation (RTE) is quite high for simulations of fires of this scale. In addition to the common three-dimensional space variables and time, the governing equation also requires integration over all directions of propagation at each point in the domain, adding two angular variables. The challenge, therefore, is to choose a numerical solution method which predicts the radiative flux to objects in fires with sufficient accuracy. Moreover, the radiative source term, which is coupled to the hydrodynamics, must be computed with low cost and sufficient accuracy to ensure a correct prediction of the evolution of the fire.

In this study, five common numerical methods to solve the radiative transfer were

† Sandia National Laboratories
‡ NASA Ames Research Center
¶ Ecole des Mines d'Albi Carmaux

compared when applied to a realistic, full-field three-dimensional fire data set. The five methods include:

1. Ray tracing: straightforward integration of the integral equation by tracing a specified number of rays originating from each point through the domain. The method is accurate but costly since it normally requires a large number of angles.

2. Discrete transfer method: similar to ray tracing technique, but works in reverse by tracing rays throughout the domain and adding their energy contribution to each cell it passes through.

3. Discrete ordinate method: solution of the transport equation by finite volume methods. The angular integration is performed using selected numerical quadrature schemes. The two quadrature shemes used were S_4 (24 angles) and LC_{11} (96 angles).

4. Moment method with the M_1 closure (Maximum entropy closure): uses moments of the governing equation to convert the angular dependence into a hyperbolic set of four equations for three-dimensional problems. A closure model is required for the radiative pressure term.

5. Monte Carlo, Net Exchange Formulation: statistical Monte Carlo method formulated in terms of net exchange and choosing a form of the probability density function for efficient computations. The cost is normally high due to the number of realizations required for good accuracy.

Of these methods, the M_1 method has theoretically the lowest cost because the angular dependency is handled analytically. However, the accuracy of the M_1 method in complex three-dimensional cases remains unknown. The main questions addressed in this study are: How does each method perform with low angular resolution? How many angles are required for an accurate solution? What is the accuracy of moment methods for fire problems? Which method is most appropriate for a fire?

2. Synthetic fire

The radiative heat transfer in large pool fires is dominated by the thermal emission of high-temperature soot and is gray in nature. Solution of the RTE in the participating medium thus requires knowledge of the gray absorption coefficient and emission temperature throughout the medium. Ideally, a complete, highly-resolved set of experimental measurements would be available for this purpose. However, due to the complex fire dynamics (Tieszen *et al.* 1996), as well as difficulty in instrumenting diagnostics in high temperature, sooting environments, relevant data for large scales fires are not available.

Given the lack of available and relevant data, a synthetic 2-meter JP-8 pool fire was created with the Vulcan fire simulation tool from Sandia National Laboratories. Vulcan, and its predecessor (Holen *et al.* 1990), has been successfully used in recent years for simulating such pool fires which resemble those in the Fire Laboratory for Accreditation of Models and Experiments (FLAME) facility in Albuquerque, New Mexico (Brown & Blanchat 2003). Figure 1 shows, from left to right: the exterior of the FLAME facility, a contour along the centerline plane of the facility showing the fuel pan in the center and the inlet air ring at the bottom of the facility; and the temperature profile of the synthetic fire along the central plane. The facility was discretized with a $92 \times 92 \times 120$ three-dimensional Cartesian grid. The full-field data is axially symmetric with the center defined by the fuel pan. In order to compute the fire, the fluid conservation equations are solved using a Reynolds Averaged Navier Stokes (RANS) approach, with sufficient iterations from ignition to reach a steady-state solution.

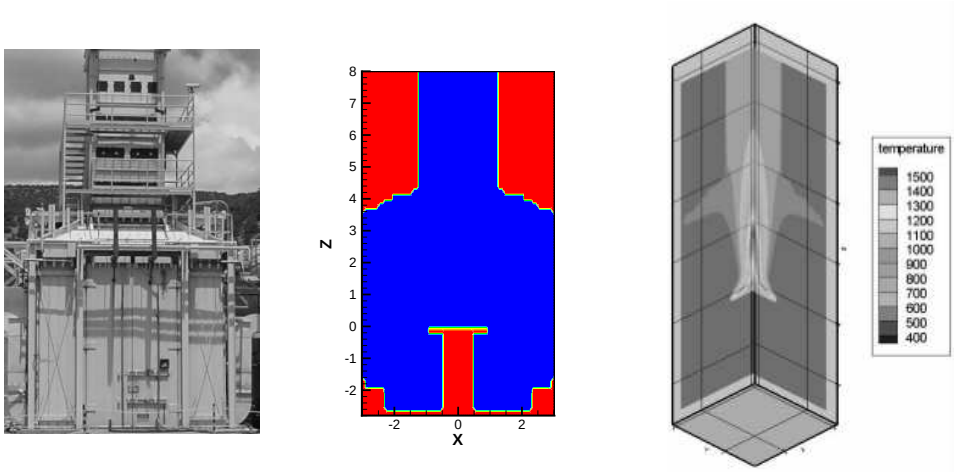

FIGURE 1. The FLAME facility (left), a contour plot of the center plane (center), and the synthetic fire temperature contour (right).

The absorption coefficients calculated by Vulcan depend on contributions from soot as well as from carbon dioxide and water vapor. The model for this coefficient assumes that the medium is gray since soot is the dominant absorbing and emitting species. When the domain of computation is as complex as the FLAME facility (see Fig. 1), prescribing common boundary conditions for five different codes can become problematic. Here, using a ghost cell technique, the walls, the pan, and the fuel source were prescribed a very large constant opacity on the order of $O(10^3)$ and ambient temperature $293\,K$. At the exhaust opening at the top of the chimney, it is assumed that all energy leaves unimpeded.

3. Solution methods for the radiative transfer equation

3.1. *Problem definition*

The gray radiative transfer equation (RTE) describes the change in radiation intensity, I, through an absorbing and emitting gray medium along a path of length ds in a solid angle $d\Omega$ (Modest 2003),

$$\frac{dI(\mathbf{s})}{ds} = \kappa I_b - \kappa I(\mathbf{s}) \tag{3.1}$$

where $I_b = \sigma T^4/\pi$ is the blackbody intensity at temperature T, σ is the Stefan-Boltzman constant, and κ is the absorption coefficient.

For most heat transfer applications, the primary engineering quantities of interest are the net incident radiation G, the radiative heat flux ($\mathbf{q}_r$) and the divergence of the heat flux ($\nabla \cdot \mathbf{q}_r$), also called radiative source term. These quantities can be derived from the following integrals of the intensity over solid angle

$$G = \int_{4\pi} I(\mathbf{s})\, d\Omega, \quad \mathbf{q}_r = \int_{4\pi} I(\Omega)\Omega\, d\Omega \quad \text{and} \quad \nabla \cdot \mathbf{q}_r = \kappa(4\sigma T^4 - G) \tag{3.2}$$

Solution of the RTE, as well as solutions of Eqs. (3.2), using each solution technique is outlined in the following subsections.

3.2. *Discrete transfer method (DTM)*

The discrete transfer method (DTM) used in Vulcan is an enhanced version of the original model proposed by Shah (1979). The enhancements were selected to obtain an acceptable compromise between accuracy and calculation speed. This will be tested by comparing the results obtained herein with those obtained from verified and highly accurate Monte Carlo and ray tracing techniques.

Within the computational domain a *radiation box* is defined to speed the calculation by focusing on the region with high thermal emission. This box defines where rays originate in the tracing technique. For this study, the box was defined as the smallest grid-conformal parallelepiped encompassing all control volumes with a temperature greater than 800 K.

For each node on the boundary of the box, a specified number of rays are emitted over a hemisphere and followed to the boundary of the calculation domain; a corresponding ray is followed back from the boundary to the original point. Along these traces, the change of intensity from absorption and emission is calculated over each control volume in the path with proper weighting given to the solid angle and the originating projected area.

The change of intensity for the ray within a control volume is found from a recurrence relation obtained from analytical integration of Eq. (3.1),

$$I_{n+1} = I_n \exp(-\kappa\delta s) + I_b(1 - \exp(-\kappa\delta s)) \tag{3.3}$$

where δs is the distance over which the beam passes through the control volume.

The source term for the energy equation, Eq. (3.2), is found by summing the net gain or loss of radiation energy in each control volume intersected during a ray trace. The contribution to the source term from one beam i passing through a control volume n is given by: $S_{n,i} = (I_{n+1} - I_n)\Omega_i \, dA \, d\Omega$, where dA is the area from the element at the ray origin boundary and Ω_i is the solid angle represented by the beam. The total radiant source term for the nth control volume is found by summing over N total beams: $Q_r \, dV = \sum_{i=1,N} S_{n,i}$

The heat flux to a surface is not calculated throughout the field of Vulcan, but rather at selected surfaces (e.g., cell faces). The hemispherical flux in $\mathrm{W/m^2}$ is derived from this model by integrating all incoming rays on a surface. This integration requires a large number of rays to be traced from each node of the radiation box to be accurate, but from experience it has been found to be quite fast when a limited number of selected surfaces are used. To compare to the other methods, the hemispherical fluxes to the common surface shared by two adjacent cells were summed for the equivalent of a 4π integration.

3.3. *Discrete ordinates method (DOM)*

The DOM is based on the discretization of the RTE (see Eq. (3.1)) over a chosen number N_{dir} of discrete directions, $\mathbf{s}_i(\mu_i, \eta_i, \xi_i)$, contained in the solid angle 4π and associated with weights w_i. Koch & Becker (2004) compare several types of angular quadratures, two of which are used here: the S_4 (24 directions) for its efficiency and the LC_{11} (96 directions) for its accuracy.

The RTE is solved for every discrete direction $\mathbf{s}_i$ using a finite volume approach. The integration of the RTE over the volume V of an element limited by a surface Σ with outer unit normal $\mathbf{n}$, and the application of the divergence theorem yield:

$$\int_\Sigma I \, \mathbf{s} \cdot \mathbf{n} \, d\Sigma = \int_V (\kappa I_b - \kappa I(\mathbf{s})) \, dV \tag{3.4}$$

The domain is discretized in control volumes (in this study regular hexahedra†). Taking I_j to be the average intensity over the j^{th} face, associated with the center of that face, and taking $I_{b,P}$ and I_P to be the average intensities over the volume V, associated with the center of the cell, P, Eq. (3.4) can be discretized as follows:

$$\sum_{j=1}^{N_{face}} I_j(\mathbf{s}_i \cdot \mathbf{n}_j)A_j = \kappa V(I_{b,P} - I_P) \tag{3.5}$$

The scalar product of the i^{th} discrete direction vector with the normal vector of the j^{th} face of the considered cell is defined by $D_{ij} = \mathbf{s}_i \cdot \mathbf{n}_j = \mu_i n_{xj} + \eta_i n_{yj} + \xi_i n_{zj}$.

I_b is assumed to be constant and equal to $I_{b,P}$ over the volume V, and I_j is taken constant over each face. For each cell, the incident radiation G, given in Eq. (3.2) is evaluated at the center by

$$G \simeq \sum_{i=1}^{N_{dir}} w_i I_P(\mathbf{s}_i) \tag{3.6}$$

For a gray medium, one obtains the divergence of the radiative heat flux using Eq. (3.2). To solve Eq. (3.5), a spatial differencing scheme based on the mean flux (DMFS), proposed by Ströhle *et al.* 2001, is used. This scheme uses the following decomposition:

$$I_P = \frac{1}{2}\overline{I_{out}} + \frac{1}{2}\overline{I_{in}} \tag{3.7}$$

where $\overline{I_{in}}$ is the weighted average of the intensities at the entering faces of the cell and $\overline{I_{out}}$ the weighted average of the intensities leaving the cell. Substituting $\overline{I_{out}}$ from Eq. (3.7) into Eq. (3.5) and after some algebra (see Joseph *et al.* 2003 for more details), one obtains:

$$I_P = \Big(\frac{1}{2}\kappa V I_b - \sum_{\substack{j \\ D_{ij}<0}} D_{ij}A_j I_j\Big) \Big/ \Big(\frac{1}{2}\kappa V + \sum_{\substack{j \\ D_{ij}>0}} D_{ij}A_j\Big) \tag{3.8}$$

After the calculation of I_P from Eq. (3.8), the radiation intensities at those cell faces at which $D_{ij} > 0$ are set equal to $\overline{I_{out}}$, obtained from Eq. (3.7).

3.4. *Monte Carlo method - net exchange formulation (MCM-NEF)*

Monte Carlo Methods (MCM) have been often used to produce highly accurate solutions in the process of validating other numerical methods (Coelho *et al.* 2003; Perez *et al.* 2004). They first appeared in the literature as strict numerical implementations of stochastic photon transport models (Hammersley & Handscomb 1967). The very large number of realizations required to achieve convergence shows the limitations of the classical Monte Carlo algorithms, particularly when optically thick media are encountered (Farmer & Howell 1994). To overcome these difficulties, a mathematical formulation using the Net Exchange Formulation (NEF) (Cherkaoui *et al.* 1996), together with adapted probability density functions, have been proposed to improve the variance reduction procedures (de Lataillade *et al.* 2002). Taking P_i as a point within the volume V_i and P_j within V_j, we denote the position vectors of P_i and P_j as $\mathbf{r}_{P_i}$ and $\mathbf{r}_{P_j}$. The net radiative exchange between two volumes V_i and V_j, $\varphi_{(V_i,V_j)}$, or a volume V_i and a surface S_j, $\varphi_{(V_i,S_j)}$, or two surfaces S_i and S_j, $\varphi_{(S_i,S_j)}$, is expressed as follows for black walls and

† the formulation provided here is also valid for non regular mesh.

non-scattering media

$$\varphi_{(V_i,V_j)} = \int_{V_j}\int_{V_i} \frac{\kappa(\mathbf{r}_{P_i})\,\kappa(\mathbf{r}_{P_j})\,\tau(s_{ij})}{s_{ij}^2}\big[I_b(\mathbf{r}_{P_i}) - I_b(\mathbf{r}_{P_j})\big]\,dV_i\,dV_j \tag{3.9}$$

$$\varphi_{(V_i,S_j)} = \int_{S_j}\int_{V_i} \frac{|\mathbf{n}(\mathbf{r}_{P_j})\cdot\mathbf{s}|\,\kappa(\mathbf{r}_{P_j})\,\tau(s_{ij})}{s_{ij}^2}\big[I_b(\mathbf{r}_{P_i}) - I_b(\mathbf{r}_{P_j})\big]\,dV_i\,dS_j \tag{3.10}$$

$$\varphi_{(S_i,S_j)} = \int_{S_j}\int_{S_i} \frac{|\mathbf{n}(\mathbf{r}_{P_i})\cdot\mathbf{s}|\,|\mathbf{n}(\mathbf{r}_{P_j})\cdot\mathbf{s}|\,\tau(s_{ij})}{s_{ij}^2}\big[I_b(\mathbf{r}_{P_i}) - I_b(\mathbf{r}_{P_j})\big]\,dS_i\,dS_j \tag{3.11}$$

where

$$s_{ij} = s_j - s_i = |\mathbf{r}_{P_j} - \mathbf{r}_{P_i}|\ ,\ \ \mathbf{s} = \frac{(\mathbf{r}_{P_j} - \mathbf{r}_{P_i})}{|\mathbf{r}_{P_j} - \mathbf{r}_{P_i}|},\ \text{ and }\ \tau(s_{ij}) = exp\Big[-\int_{s_i}^{s_j}\kappa(s)ds\Big] \tag{3.12}$$

with $\mathbf{n}$ the normal vector to the surface S, κ the gray absorption coefficient, and $\tau(s_{ij})$ is the spectral transmittance along a straight line between P_i and P_j.

The radiative source term for a volume V_i and the net heat flux at a surface S_i are computed by taking into account their radiative exchanges with all the other volumes and surfaces:

$$S_r(\mathbf{r}_{P_i}) = \int_{V_i}\nabla\cdot\mathbf{q}_r\,dV_i = \sum_{j=1}^{N_s}\varphi_{(V_i,S_j)} + \sum_{j=1}^{N_v}\varphi_{(V_i,V_j)} \tag{3.13}$$

and

$$q_{w,net,i} = \sum_{j=1}^{N_s}\varphi_{(S_i,S_j)} + \sum_{j=1}^{N_v}\varphi_{(S_i,V_j)} \tag{3.14}$$

where N_s is the number of surfaces and N_v the number of volumes.

One way of evaluating the multiple integrals in the expressions for the net exchange rates, Eqs. (3.9), (3.10), (3.11), is to use a Monte Carlo Method, which is now described.

Considering that each radiative exchange can be represented as an integral $\mathcal{I}$, of a function f, over a domain D: $\mathcal{I} = \int_D f(x)dx$. An arbitrary probability density function (pdf), p, defined and strictly positive on the integration domain D is introduced. The weight function $W(x) = f(x)/p(x)$ is used to write

$$\mathcal{I} = \int_D \frac{f(x)}{p(x)}p(x)dx = \int_D W(x)p(x)dx$$

Given a random variable X, distributed according to p, and a function of that variable, $g(X)$, we let $\mathcal{I}$ represent the expectation of $g(X)$. Estimating $\mathcal{I}$ with N samples $g(x_i)$, where x_i is the ith realization of the random variable X gives

$$\mathcal{I} = E[g(X)] \approx \frac{1}{N}\sum_{i=1}^{N} g(x_i) =< g(X) >_N, \quad \text{where } \mathcal{I} = \lim_{N\to\infty} < g(X) >_N \tag{3.15}$$

Then the standard deviation of the estimate is calculated as $\sigma(< g(X) >_N) = \frac{1}{\sqrt{N}}\sigma(g(X))$, where $\sigma(g(X))$ is the standard deviation of $g(X)$. It will be approximated by

$$\sigma(< g(X) >_N) \approx \frac{1}{\sqrt{N}}\sqrt{[< g(X)^2 >_N - < g(X) >_N^2]} \tag{3.16}$$

In this last expression the variance depends on the function g which itself depends on the

pdf. To perform efficient MC simulations, the choice of the pdf is crucial. More details are described in (de Lataillade *et al.* 2002; Eymet *et al.* 2004). The results presented in this paper have a standard deviation of about 1 percent.

3.5. *Ray tracing method*

This method treats the RTE as a set of first-order ODEs, with one ODE for each spatial point and directional angle. At each spatial point $\mathbf{x}$, a set of rays is considered to project inward toward the point, with the set being chosen to sample solid angle space in such a way as to allow accurate integration over that space to compute the net incident radiation and the heat flux. For the fire problem, the rays are followed outward from the chosen point until they intercept a wall or the exit of the chimney. At such a boundary point the initial value of the incoming radiative intensity is set to equilibrium ($I = I_b$). From this initial value, the RTE is integrated forward along the ray to the chosen spatial point, and the value at that point is saved for inclusion in angular integrals involving $I(\mathbf{x}, \Omega)$.

The method of integration along a ray assumes that, within each step of the quadrature, the source I_b and opacity κ are constants equal to their interpolated values at the center of the step. With this assumption, $I(\mathbf{s}, \Omega)$ can be advanced from one end of the step, $\mathbf{s}_0$, to the other, $\mathbf{s}_1$, according to the following rule

$$I(\mathbf{s}_1, \Omega) = I(\mathbf{s}_0, \Omega) \exp(-\kappa|\mathbf{s}_1 - \mathbf{s}_0|) + I_b(1 - \exp(-\kappa|\mathbf{s}_1 - \mathbf{s}_0|)) \tag{3.17}$$

Once the full set of angular values $I(\mathbf{x}, \Omega)$ is obtained at the point $\mathbf{x}$, angular integrals, such as those in Eqs. (3.2), are performed to compute quantities of interest.

3.6. *Moment methods and the* $\mathbf{M_1}$ *closure*

A system of equations for two moments, the net incident radiation G and the radiative flux $\mathbf{q}_r$, can be extracted from the gray RTE, Eq. (3.1), by integrating it over all directions. The system is given by

$$\frac{1}{c}\partial_t G + \nabla \cdot \mathbf{q}_r = \kappa(4\sigma T^4 - G) \tag{3.18}$$

$$\frac{1}{c}\partial_t \mathbf{q}_r + \nabla \cdot (\mathbf{D}_r\ G) = -\sigma\ \mathbf{q}_r \tag{3.19}$$

The M_1 closure (Levermore 1984; Fort 1997†) is given by the following Eddington tensor $\mathbf{D}_r$. It is computed from the Eddington factor χ and the anisotropic factor $\mathbf{f} = \mathbf{q}_r/G$ as follows

$$\mathbf{D_r} = \frac{1-\chi}{2}\ \mathbf{Id} + \frac{3\chi - 1}{2}\ \frac{\mathbf{f} \otimes \mathbf{f}}{f^2} \quad \text{with} \quad \chi(f) = \frac{3 + 4f^2}{5 + 2\sqrt{4 - 3f^2}} \tag{3.20}$$

where $\mathbf{Id}$ denotes the identity matrix, f the euclidian norm of $\mathbf{f}$, and $\otimes$ the dyadic product. The Eddington tensor $\mathbf{D}_r$, which plays the role of a flux limiter, comes from an underlying radiative intensity which is able to describe both a beam (by a Dirac function) as well as isotropic radiation (by a Planck function). Hence, the M_1 model is able to predict radiation in opaque, semi-opaque or transparent media and, as we show below, is particularly suited for the computation of radiation in fires. The numerical scheme used to solve this model is given in Ripoll *et al.* 2002.

† more references concerning this model can be found in Ripoll 2004.

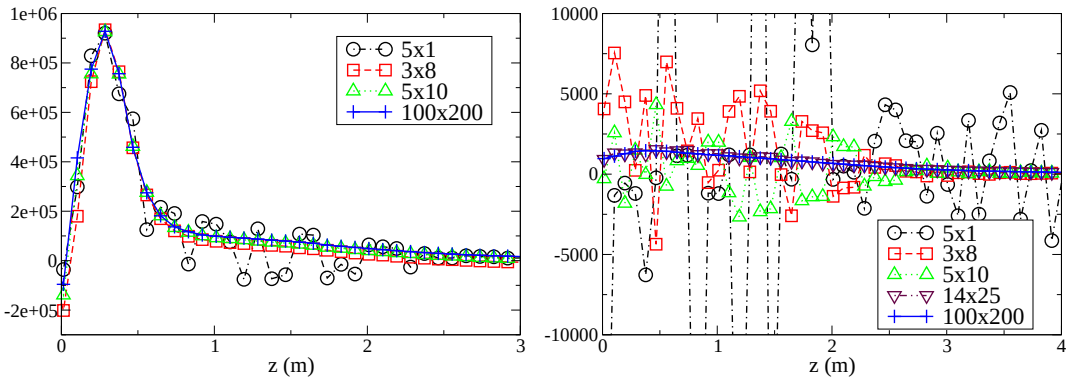

FIGURE 2. Radiative source term (W/m^3) at $r = 0.43\,\mathrm{m}$ (left) and radial heat flux (W/m^2) at $r = 1.03\,\mathrm{m}$ (right) as a function of elevation from the fuel pan computed by ray tracing for several angular resolutions (θ, ϕ).

4. Results and discussion

4.1. *Angular resolution and coupling*

In this section, the number of angles (or rays) needed for the fire computation is investigated using the ray tracing code, which helped define the required angular resolution and quadrature schemes for comparison of the solution methods. Figures (2) and (3) (left) show the radiative source term and radial heat flux profiles calculated at various angular resolutions. It is found that a low resolution, less than 50 angles, leads to poor results both inside and outside the fire. When only 5 or 10 angles are used, a hot source might be hit or not according to the angles chosen, in other words, ray effects are dominant and the results vary greatly based on this choice.

Inside the fire, it is found that at least 50 rays are needed to get a solution close to the converged one† (see Fig. 2). However outside the fire, Fig. 3 (left), it is found that 350 angles are needed to get an acceptable solution and to reduce ray effects. Hence, because such resolutions are needed for accuracy, a high computational cost is expected. Nevertheless, these results must be balanced by the fact that neither special quadratures, nor particular choices of angles have been used herein to try to improve the accuracy of the results for low angular resolution. In the ray tracing solver, angles are uniformly distributed in $\mu = \cos(\theta)$ and ϕ, which is not the optimal choice. Undoubtedly a better choice of angles and/or quadratures would decrease the number of angles needed to get accurate results‡.

In Fig. 3 (right), it is shown how the angular resolution does affect the time-dependent coupled problem. Here, radiation and hydrodynamics are solved coupled by Vulcan and evolve in time. Radiation is solved by the DTM method. It is found that 24 angles do not lead to an accurate solution and induce strong temporal variation of the radiative flux, which leads to fluctuations in the hydrodynamic quantities. Moreover, since the coupling between radiation and hydrodynamics is very strong in fires, a poor computation of the

† Angular convergence was obtained with 20,000 angles (100 × 200). All results presented with the RTE ray tracing solver in this study were obtained with this resolution.

‡ The reader might be interested in seeing which angular quadrature is needed for radiation in a solar atmosphere: Stein *et al.* in this volume.

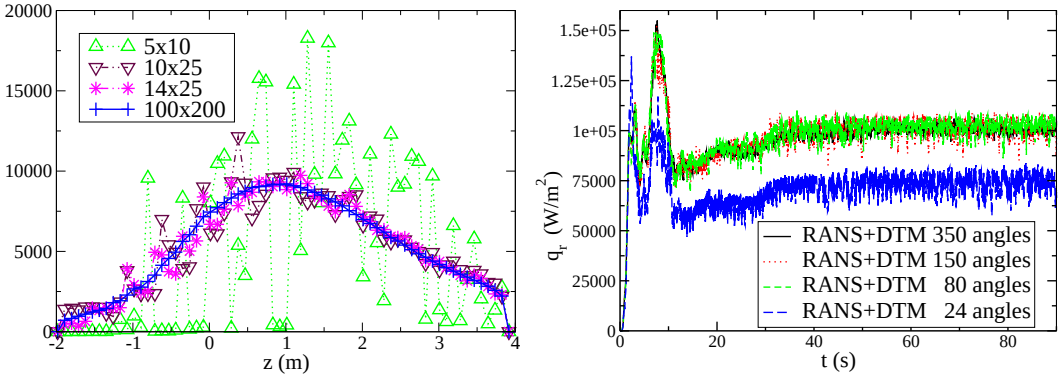

FIGURE 3. Left: Radial component of the radiative flux (W/m^2) as a function of elevation from the fuel pan computed by ray tracing for different resolutions (θ, ϕ) at $r = 2.55$ m from the centerline of the fuel pan. Right: time evolution profiles of the radial component of the radiative flux at $r = 0.5$ and $z = 0.5$ m inside the fire for several angular resolutions using DTM.

radiation can, for instance, lead to extinction or to an over/under-estimation of soot formation.

Starting from 80 angles, which seems to be a good compromise between speed and accuracy, the Vulcan results are close to convergence, but the fluctuations are still significant. Results are considered converged for a resolution of 350 angles. As a result of these observations, the code is usually run with 80 angles to quickly obtain a fully developed fire. The results are converged afterward using 350 angles over a smaller time interval†.

4.2. *Radiative source term*

A comparison of the radiative source terms ($div(\mathbf{q}_r)$) obtained by all methods‡ is now provided. Since this quantity is the coupling term used by the hydrodynamics solver, its accurate computation is mandatory to compute the correct final fire profile. The ray tracing code and the Monte Carlo code are used for the reference solutions¶. Both codes find similar solutions at all points in the facility. In Fig. 4 (left), the results are presented for points inside the fire. Good global agreement is found between all methods, though the DTM profile is slighty shifted from the ray tracing reference solution; DTM, M_1, and DOM S_4 slightly overestimate the maximum value, and DOM LC_{11} slightly underestimates it. These small differences of less than 3% are sufficiently small to not have strong effects on the coupled energy equation. The accuracy and general agreement between these results is expected for this case where the radiation field inside the fire is mainly isotropic, $f < 0.2$, making it less sensitive to angular resolution.

For points outside, but still adjacent to, the fire, at $r = 1.15\,m$ (see Fig. 4 (right)), more discrepancies are seen among the methods‖. The DOM S_4 method is found to be less accurate, though still acceptable, compared to the DOM LC_{11} because the angular

† All results presented here with the DTM have been obtained with 350 angles.

‡ when this term is positive (negative), net emission (absorption), is occurring.

¶ The Monte Carlo code was primarly used to ensure that the solution given by the ray tracing was fully correct. It has been applied only at selected positions and not for all nodes of the domain.

‖ a large error far outside the fire would not affect the dynamics of the fire and is hence not damaging.

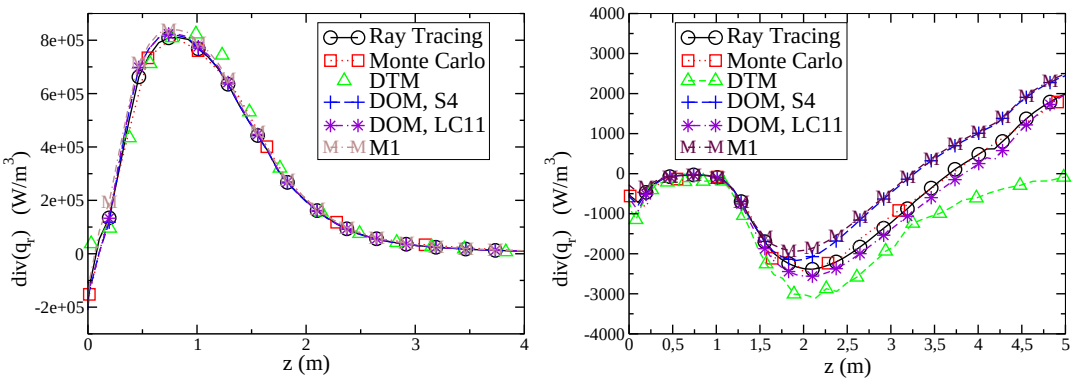

FIGURE 4. Radiative source term (W/m^3) as a function of elevation from the fuel pan. Left at $r = 0.29\,\mathrm{m}$ and right at $r = 1.15\,\mathrm{m}$ from the centerline of the fuel pan.

variation is not fully captured by S_4 and ray effects occur. The M_1 model gives results as accurate as those of the DOM S_4, which is encouraging. These methods slightly underestimate absorption while the DTM method overestimates it. Despite the discrepancies, the magnitude of the source term is sufficiently small compared to that inside the fire that less accuracy is acceptable.

4.3. *Radial heat flux*

Since the Monte Carlo code, by its formulation, does not allow the computation of the radiative fluxes which are compared herein, the ray tracing results are used as the reference. In Figs. 5 and 6, net radial heat flux inside the fire are compared. All methods qualitatively agree and predict the same trends. Higher up, for $z > 1.5\,m$, all methods fully agree since strong temperature and opacity gradients are absent. The three methods, M_1, S_4 and LC_{11} are in good agreement with the reference solution, but slightly underestimate the flux. The DTM method agrees globally with the other methods and the reference solution, but overestimates slightly, similar to LC_{11}, fluxes close to the outer edge of the fuel pan at $r = 1$ and $z = 0\,m$. Similarly to the source term computation, the M_1 and S_4 methods give comparable results. No noticeable difference is observed between S_4 and LC_{11}, whose results agree well with those of the ray tracing method.

The fact that S_4 computes both flux and source terms relatively well, when linked with the angular studies of section 4.1, implies that 24 angles should be enough inside the fire provided that the S_4 set of angles is chosen. This constitutes an improvement by a factor of two of the number of angle needed, compared to the use of uniformly distributed angles†.

In Fig. 7, the fluxes outside the fire are compared. The DTM method gives results in agreement with the ray tracing solver. The DOM LC_{11} gives similar results, which suggest that approximately a hundred angles should be enough to compute radiation at 1 or 2 diameters away from the fire provided an accurate quadrature is chosen. This constitutes an impromentby a factor 3 compared to a uniformly spaced angular set which apparently needs 350 angles (see section 4.1). The DOM S_4 does not have enough angular

† It should be noted that the 24 angles of DTM used in the time evolution computation are uniformly distributed. This explains the inaccurate results of the time dependent problem for this angular resolution.

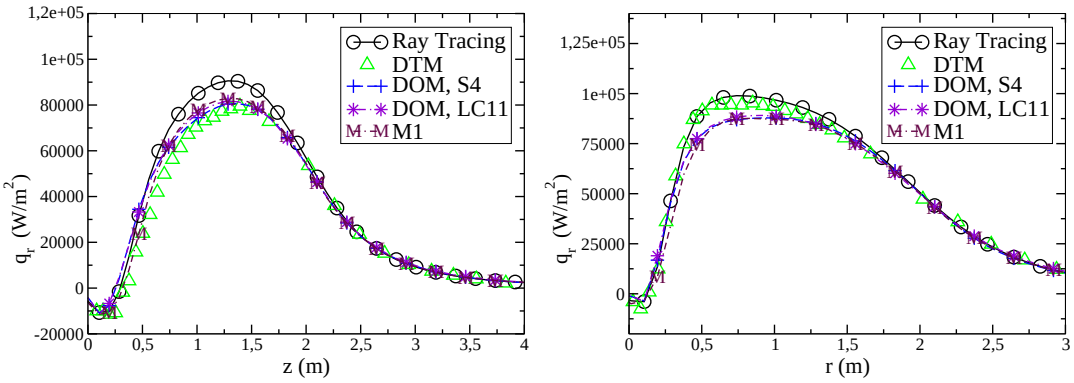

FIGURE 5. Radial component of the radiative flux (W/m^2) as a function of elevation from the fuel pan. Left at $r = 0.29$ m and right at $r = 0.42$ m from the centerline of the fuel pan.

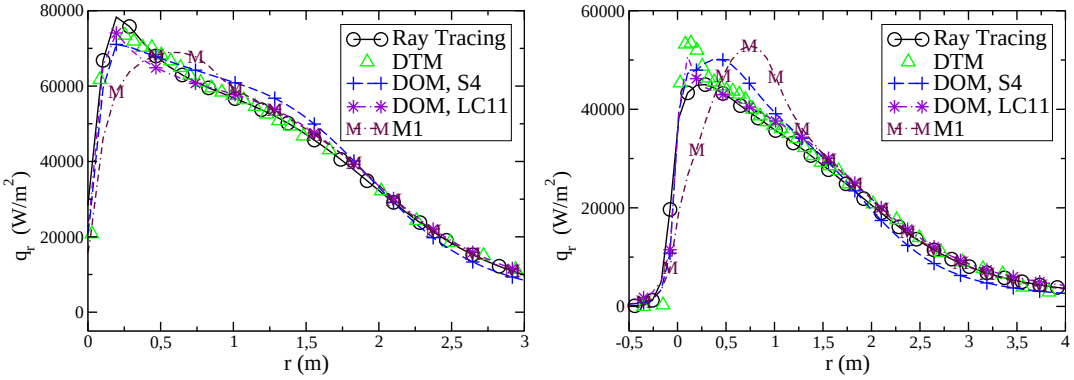

FIGURE 6. Radial component of the radiative flux (W/m^2) as a function of elevation from the fuel pan. Left at $r = 0.7$ m and right at $r = 1.03$ m from the centerline of the fuel pan.

resolution to provide accurate results at 1.42 m nor at 2 m away from the fire. LC_{11} thus constitutes an accuracy improvement compared to S_4. Globally, this method is found to give the closest results to the ray tracing values for all positions shown here. The M_1 model is found here to not be accurate enough: results at 1.42 m could be admissible, but the fluxes are certainly overestimated 2 m away from this 2 m pool fire, by almost a factor of 2. There, the closure fails to model the anisotropy of the radiation. At 2 m, DOM S_4 computes the maximal values more accurately than M_1, but does not find the correct overall shape‡, whereas M_1 does.

5. Conclusions

Five different methods have been used to compute the radiative field of a synthetic 2-meter JP-8 pool fire: Monte Carlo, ray tracing, DOM S_4 and LC_{11}, DTM, and the M_1 moment model. Particular interest has been given to the M_1 method which is applied for the first time to a combustion problem occurring in a complex three-dimensional

‡ a ray effect can been seen at $z = 0.1\,m$ due to the pan.

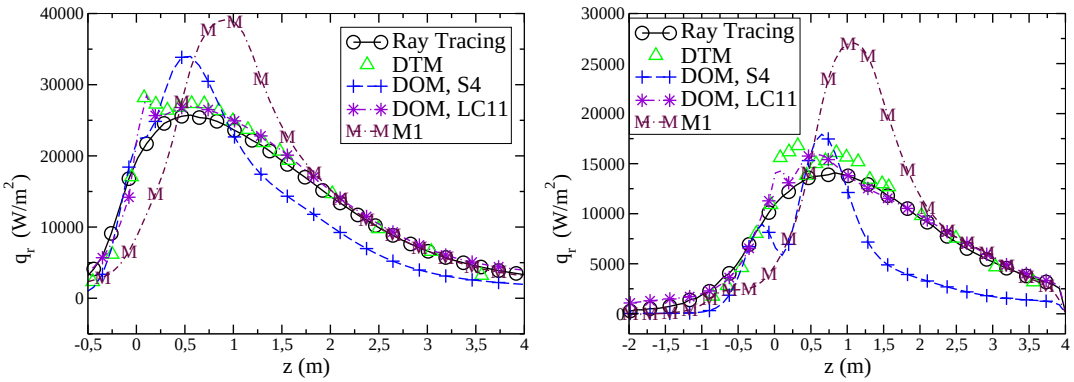

FIGURE 7. Radial component of the radiative flux (W/m^2) as a function of elevation from the fuel pan. Left at $r = 1.42$ m and right at $r = 2$ m from the centerline of the fuel pan.

geometry. Theoretically, this model should have the lowest computational cost of the five, since the directional integration has been modeled.

An angular resolution study has shown that roughly 50 angles inside and 350 outside the fire are needed to accurately compute radiation when a uniformly distributed set of angles is chosen. This choice of angles is not optimum, however, and the number of angles needed can be reduced to 24 inside and to roughly 100 outside when an optimum set is chosen, as is the case for both the S_4 and LC_{11} quadratures. Unfortunately, these numbers are still too high to guarantee a low cost computation. It has also been shown that if an insufficient angular distribution is used, then significant changes to the time dependent solution occur. It is thus not possible to accurately compute a time-evolving fire if the aforementioned angular requirements are not satisfied.

The ray tracing and Monte Carlo methods, which are the most accurate methods when their convergence is ensured, and the results of which were found to be consistent, were used to compute the reference solutions. Both of these methods, which need, respectively, a large number of angles or a large realization sample, are too costly to be used for a three-dimensional time dependent fire. The goal was then to quantify the accuracy of the four other methods, compared to the reference solutions, and to assess their usability.

The five methods were compared first through the computation of the radiative source term. It was found that, inside the fire, all methods correctly compute this term, which is needed for coupling with the hydrodynamics. Close to the fire, this term is underestimated by S_4 and M_1 and overestimated by DTM, but these deviations of less than 3% are quite admissible.

The computation of the radiative flux brought other conclusions. Inside the fire, all methods agree pretty well. Once again, M_1 gives a comparable solution to the DOM methods. However, outside the fire both S_4 and M_1 methods inaccurately compute the flux: S_4 suffers from ray effects and M_1 overestimates, by almost a factor two, the maximal value region. These two methods are thus not effective far away from the fire. On the other hand, LC_{11} and DTM give an accurate solution far away the fire, but deviate slightly close to the outer edge of the fuel pan.

Overall, it is found that M_1 gives results similar to DOM S_4, in the sense that its results are accurate in regions where S_4 is accurate. The DTM and DOM LC_{11} methods were found to give results very close to the Monte-Carlo and ray tracing codes. The

comparison of the accuracy and speed of the five solution methods suggest that the M_1 model is a good alternative to S_4 when solving the RTE in complex cases such the large pool fire in this study. For the limited case where highly-accurate heat flux in the highly anisotropic area, e.g., the flux to an object a few diameters away from the fire, better accuracy is only achieved with higher angular resolution offered by DOM LC_{11} or a large number of angles using ray tracing or the DTM method.

Acknowledgments

The authors thank Dr. Sheldon Tieszen of Sandia National Laboratories for his extensive technical discussions and support. Kirk Jensen was supported by the Advanced Simulation and Computing Program of Sandia, a multi-program laboratory operated by Sandia Corporation, a Lockheed-Martin Company, for the United States Department of Energy's National Nuclear Safety Administration under Contract DE-AC04-94AL85000.

REFERENCES

Brown, A.L., & Blanchat, T.K. 2003 A validation quality heat flux dataset for large pool fires. *2003 ASME Summer Heat Tansfer Conference, Las Vegas HT2003-40249.*

Cherkaoui, M., Dufresne, J.L., Fournier, R., Grandpeix, J.Y. & Lahellec, A. 1996 Monte Carlo simulation of radiation in gases with a narrow-band model and a net-exchange formulation. *Jour. of Heat Transfer* **118**, 401-407.

Coelho, P.J., Perez, P. & El Hafi, M. 2003 Benchmark numerical solutions for radiative heat transfer in two-dimensional axisymmetric enclosures with non-grey sooting media. *Numerical Heat Transfer, Part B*, **43**, 425-444.

de Lataillade, A., Dufresne, J.L., El Hafi, M., Eymet, V. & Fournier, R. 2002 A net exchange Monte Carlo approach to radiation in optically thick systems. *Jour. of Quant. Spectrosc. & Radiat. Transfer*, **74:5**, 563-584.

Eymet, V., Fournier, R., Blanco, S. & Dufresne, J.L. 2004 Boundary-based net exchange Monte-Carlo method for absorbing and scattering thick media. *Jour. of Quant. Spectrosc. & Radiat. Transfer*, in press.

Farmer, J.T. & Howell J.R. 1994 Hybrid Monte Carlo/ diffusion method for enhanced solution of radiative transfer in optically thick non-gray media. *Radiative Transfer: Current Research, Y. Bayazitloglu et al., eds. ASME*, **276**, 203-212.

Fort, J. 1997 Information-theoretical approach to radiative transfer. *Phys. A.*, **243**, 275-303.

Gritzo, L.A., Sivathanu, Y.R., & Gill, W. 1998 Transient measurements of radiative properties, soot volume fraction and soot temperature in a large pool fire. *Combustion Science and Technology* **84**, 113-136.

Hammersley, J.M. & Handscomb, D.S. 1967 *Monte Carlo Methods.* Dunod, Monographie.

Holen, J., Brostrom, M., & Magnussen, B.F. 1990 Finite difference calculation of pool fires. *Twenty-Third Symposium (International) on Combustion, The Combustion Institute*, 1677-1683.

Joseph, D., Coelho, P.J., El Hafi, M. & Cuenot, B. 2003 Application of the discrete ordinates method to grey media in complex geometries using unstructured meshes. *Proceedings of Eurotherm73 on Computational Thermal Radiation in participating media, Eurotherm Series* **11**, 97-106.

KOCH, R. & BECKER, R. 2004 Evaluation of the quadrature schemes for the discrete ordinates method. *Jour. of Quant. Spectrosc. & Radiat. Transfer.*, **84**, 423-435.

LEVERMORE, D. 1984 Relating Eddington factors to flux limiters. *Jour. of Quant. Spectrosc. & Radiat. Transfer*, **32(2)**, 149-160.

MODEST, M.F. 2003 Radiative heat transfer. 3rd ed., McGraw-Hill.

PEREZ, P., EL HAFI, M. COELHO, P.J. & FOURNIER R. 2004 Accurate solutions for radiative heat transfer in two-dimensional axisymetric enclosures with gas radiation and reflective surfaces. Accepted in *Numerical Heat Transfer, Part B.*

RIPOLL, J.-F. 2004 An average formulation of the M_1 radiation model with mean absorption coefficients and presumed probability functions for turbulent flows. *Jour. of Quant. Spectrosc. & Radiat. Transfer*, **83**, 493-517.

RIPOLL, J.-F., DUBROCA, B., AUDIT, E. 2002 A factored operator method for solving coupled radiation-hydrodynamics models. *Trans. Theory and Stat. Phys.*, **31**(4-6), 531-557.

SHAH, N.G. 1979 The computation of radiation heat transfer. *PhD thesis, University of London.*

STRÖHLE, J., SCHNELL, U. & HEIN, K.R.G. 2001 A mean flux discrete ordinates interpolation scheme for general coordinates. *3rd International Conference on Heat Transfer, Antalya.*

TIESZEN, S.R., NICOLETTE, V.F., GRITZO, L.A., HOLEN, J.K., MURRAY, D., & MOYA, J.L. 1996 Vortical structures in pool fires: observation, speculation, and simulation. *SAND Report No. SAND96-2607, Sandia National Laboratories.*